Article

Dithiothreitol-Regulated Coverage of Oligonucleotide-Modified Gold Nanoparticles to Achieve Optimized Biosensor Performance

Pingping Liang, Juan Canoura, Haixiang Yu, Obtin Alkhamis, and Yi Xiao

ACS Appl. Mater. Interfaces, **Just Accepted Manuscript** • DOI: 10.1021/acsami.7b16914 • Publication Date (Web): 09 Jan 2018

Dithiothreitol-Regulated Coverage of Oligonucleotide-Modified Gold Nanoparticles to Achieve Optimized Biosensor Performance

Pingping Liang, Juan Canoura, Haixiang Yu, Obtin Alkhamis and Yi Xiao*

Department of Chemistry and Biochemistry, Florida International University, 11200 SW 8th Street, Miami, FL, 33199.

*Corresponding author: yxiao2@fiu.edu

ABSTRACT

DNA-modified gold nanoparticles (AuNPs) are useful signal-reporters for detecting diverse molecules through various hybridization- and enzyme-based assays. However, their performance is heavily dependent on the probe DNA surface coverage, which can influence both target binding and enzymatic processing of the bound probes. Current methods used to adjust surface coverage of DNA-modified AuNPs require the production of multiple batches of AuNPs under different conditions, which is costly and laborious. We here develop a single-step, rapid, and reproducible assay utilizing dithiothreitol (DTT) to fine-tune the surface coverage of DNA-modified AuNPs. DTT is superior to the commonly used surface diluent, mercaptohexanol, as it is less volatile, allowing for the rapid and reproducible fine-tuning of surface coverage on AuNPs with only micromolar concentrations of DTT. Upon adsorption, DTT forms a dense monolayer on gold surfaces, which provides anti-fouling capabilities. Furthermore, surface-bound DTT adopts a cyclic conformation, which reorients DNA probes into an upright position and provides ample space to promote DNA hybridization, aptamer assembly, and nuclease digestion. We demonstrate the effects of surface coverage on AuNP-based sensors by using DTT-regulated DNA-modified AuNPs. We then use these AuNPs to visually detect DNA and cocaine in colorimetric assays based on enzyme-mediated AuNP aggregation. We determine that DTT-regulated AuNPs with lower surface coverage achieve shorter reaction times and lower detection limits relative to assays using untreated AuNPs or DTT-regulated AuNPs with high surface coverage. Additionally, we demonstrate that our DTT-regulated AuNPs can perform cocaine detection in 50% urine without any significant matrix effects. We believe that DTT regulation of surface coverage can be broadly employed to optimize DNA-modified AuNP performance for use in biosensors as well as drug delivery and therapeutic applications.

KEYWORDS: Gold nanoparticles, DNA surface coverage, dithiolthreitol, enzyme-assisted target recycling, DNA detection, cocaine detection

INTRODUCTION

Gold nanoparticles (AuNPs) functionalized with thiolated oligonucleotides can be used to selectively detect diverse targets.[1–3] Applications for such particles to date have included bioimaging, diagnostic assays, and nanometer-scale assembly.[4–8] In particular, DNA-modified AuNPs have served as useful reporters for colorimetric detection based on their high extinction coefficients and sensitive inter-particle-distance-dependent absorption spectra.[9,10] A number of groups have developed methods based on enzymatic processing as a strategy for achieving naked-eye detection of various targets with DNA-modified AuNPs.[11,12] In these methods, targets can mediate either enzyme-assisted aggregation[11] or dissociation[12] of DNA-modified AuNPs, resulting in a visible color change. One commonly-employed strategy known as "dissociation-to-aggregation" has been used for the detection of metal ions[11], enzyme inhibitors[13], DNA[11], and even DNA methylation[13]. In general, DNA-modified AuNPs are stable in high ionic strength buffers due to repulsion by the negatively-charged DNA strands tethered to the particle surface.[11,13] These surface-bound DNA strands are subsequently removed by a target-triggered enzymatic cleavage reaction. The resulting reduction of negative charge destabilizes the AuNPs and causes them to aggregate, producing a visible color change.[11,13] As an example, we have previously exploited the selectivity of exonuclease III (Exo III) for DNA duplexes in enzyme-assisted target recycling (EATR) assays to achieve amplified and rapid naked-eye detection of DNA.[14] When the DNA target is present, Exo III rapidly cleaves the hybridized probes off of the nanoparticles, producing a color change due to particle aggregation. This color change does not occur in the absence of target. This sensor platform has also been adapted to detect non-nucleic acid targets by using aptamers, which are single-stranded oligonucleotide bio-receptors isolated *in vitro* through systematic evolution of ligands by exponential enrichment (SELEX).[15,16] We recently engineered a cooperative-binding split aptamer (CBSA) containing a pair of target-binding domains that can bind cocaine with high affinity[17] and used it to achieve EATR-mediated visual detection of the drug.

The performance of DNA-modified AuNP-based colorimetric sensors is highly dependent on the extent of DNA probe surface coverage.[18–20] At low surface coverages, the probes are separated by large distances, resulting in minimal repulsion between DNA strands and high probe flexibility. The flexible DNA probes interact with the surface via their nitrogenous bases,[21-23] which renders them unavailable for base-pairing with DNA targets.[18-20] At high surface coverages, probe DNA strands are oriented in an upright position perpendicular to the surface due to the high steric and electrostatic repulsion between adjacent DNA probes.[21-23] These repulsive forces make interactions with complementary oligonucleotides difficult, which results in poor hybridization efficiency.[18-20] Furthermore, the density of probe DNA greatly affects enzyme-mediated DNA elongation[20] or cleavage[24] on the particle surface. For example, one study found that AuNP-immobilized DNA molecules resist DNase I degradation at high probe densities.[24] This was attributed to the high concentration of negatively-charged DNA phosphates on the surface of the AuNPs, which resulted in a higher local salt concentration, inhibiting enzymatic activity. Since hybridization efficiency and enzymatic activity are critical determinants of sensor performance, it is essential to maintain close control over DNA surface coverage in AuNP-based assays.

The current methods used to control DNA surface coverage on AuNPs entail adjusting buffer ionic strength,[25] the concentration of thiolated probe-DNA,[26] and/or the amount of surface diluent used during the modification step.[19] However, large-scale parallel modification of AuNPs under different conditions must be performed to obtain particles with various surface coverages, which is costly and laborious.

Alternatively, the surface diluent dithiothreitol (DTT) can be used to rapidly and reproducibly control the surface coverage of AuNPs. DTT has several favorable attributes to fine-tune the surface coverage for optimization of AuNP-based sensors. First, it is not very volatile, therefore micromolar concentrations of DTT can be accurately prepared and employed to control DNA surface coverage on the particles. Second, DTT adsorbs irreversibly on gold surfaces via its two sulfhydryl groups within minutes.[27] Third, the assembled DTT molecules are mainly in a cyclic configuration[28] which provides free space to facilitate efficient interaction of biomolecules with immbolized oligonucleotides on the particle surface. In this work, we have demonstrated that AuNP-based EATR-mediated colorimetric assays can be rapidly optimized by regulating the surface coverage of DNA-modified AuNPs with DTT. Specifically, a single batch of modified AuNPs with saturating surface coverage were treated with various micromolar concentrations of DTT to displace DNA strands and produce AuNPs with different surface coverages in only one step. We first systematically studied the displacement kinetics and surface coverage of probe DNA as a function of the concentration of DTT. We then used these DTT-regulated AuNPs in AuNP-reported EATR-based colorimetric assays and determined that optimization of DNA surface coverage dramatically improved sensor detection time, dynamic range, and detection limit for the detection both DNA and cocaine. We attribute this enhanced sensor performance to improved DNA-probe hybridization, aptamer-target assembly, and nuclease activity at the AuNP surface. We believe that DTT can be used generally to rapidly regulate the surface coverage for optimizing the performance of various AuNP-based applications.

EXPERIMENTAL SECTION

Materials. SYBR Gold and OliGreen were purchased from Invitrogen. *E. coli* Exonuclease III was acquired from New England Biolabs. Unless otherwise specified, all other reagents were obtained from Sigma-Aldrich. HPLC-purified oligonucleotides were obtained from Integrated DNA Technologies, and diluted to 250 μM in PCR quality water. The concentrations of the DNA solutions were measured using a NanoDrop 2000 spectrophotometer (Thermo Scientific). The following DNA sequences were used in this work (/iSpC3/ denotes a C_3 spacer abasic site, FAM denotes a fluorescein modification):

1X-DNA: 5' HS-$(CH_2)_6$ TTT TTT ACC ACA TCA TCC - /iSpC3/ - TAT AAC TGA AAG CCA AAC AG-3'

1X-FAM-DNA: 5' HS-$(CH_2)_6$ TTT TTT ACC ACA TCA TCC -/iSpC3/-TAT AAC TGA AAG CCA AAC AG-FAM-3'

DNA Target: 5'-CTG TTT GGC TTT CAG TTA TAT GGA TGA TGT GGT-3'

CBSA-SF: 5'-GAG ACA AGG - /iSpC3/- GAC AAG GAG-3'

SH-CBSA-SF: 5' HS-$(CH_2)_6$-TTT TTT GAG ACA AGG - /iSpC3/- GAC AAG GAG-3'

CBSA-LF: 5'-CTC CTT CAA CGA AGT GGG TCT CCT TCA ACG AAG TGG GTC TC-3'

Dithiothreitol (DTT) treatment for regulating surface coverage of DNA-modified AuNPs. DNA-AuNP conjugates were prepared via gold-sulfur chemistry as previously reported.[29] Briefly, DNA was reduced using tris(2-carboxyethyl) phosphine (TCEP) (final concentration 3.0 μM) and mixed with 3 mL of freshly prepared 10 nM 13-nm citrate-coated AuNPs[30] and incubated at room temperature for 40 hrs. During modification, 0.3 M NaCl was used to age the DNA-modified AuNPs. Following modification, the DNA-modified AuNPs were centrifuged to remove unbound DNA and 10 mM Tris buffer (pH 7.4) was used to wash the particles. After separation, the AuNPs were resuspended in 10 mM Tris buffer and stored at 4 °C. For the DTT regulation process, we mixed 55 μL of 5 nM modified AuNPs with 22 μL of

solution containing DTT at various micromolar concentrations, which had been dissolved in 10 mM Tris buffer. The mixtures were then incubated for half an hour at 25 °C. Excess DTT and removed DNA were then removed via centrifugation at 25,000 rcf and the supernatant was discarded. Then, 100 μL of 10 mM Tris buffer was used to wash the DTT-treated AuNPs twice. The particles were subsequently resuspended in the same buffer. Kinetic measurements of DTT displacement using 1X-FAM-DNA-modified AuNPs were performed by mixing 10 μL of various concentrations of DTT with 25 μL of the 5 nM modified AuNP solution. The fluorescence intensities were immediately recorded for 60 minutes at a 520-nm emission wavelength, with excitation at 495 nm.

Surface coverage characterization of FAM-labeled DNA-modified AuNPs. The surface coverage of DTT-regulated, 1X-FAM-DNA-modified AuNPs was determined with a previously reported assay.[25] 10 μL of DTT-treated, 1X-FAM-DNA-modified AuNPs were diluted to 50 μL. The absorbance of the solution was measured at 520 nm with a Tecan Infinite M1000 PRO. Beer's law was used to calculate the concentration of AuNPs ($\varepsilon = 2.7 \times 10^8$).[31,32] 50 μL of 1 M DTT in 10 mM Tris (pH 7.4) was then added to the AuNP solution, which was then incubated for 18 hours at 25 °C. This incubation was sufficient to allow complete displacement of immobilized 1X-FAM-DNA molecules from the AuNP surface. Following incubation, the solution was subjected to centrifugation for 10 minutes at 25,000 rcf, after which the supernatant was collected and transferred into a 384-well microplate. Then the fluorescence intensity was measured at 520 nm (λ_{ex}= 495 nm). A standard calibration curve was established by using known concentrations of 1X-FAM-DNA diluted with 10 mM Tris buffer (pH 7.4) and combined with the same volume of 1 M DTT. Calibration curve samples underwent the same incubation and centrifugation procedures employed for the 1X-FAM-DNA-modified AuNP samples. The surface coverage was calculated by dividing the supernatant DNA concentration by the AuNP concentration, with the resulting value reported as the average amount of DNA strands per particle.

Surface coverage characterization of unlabeled DNA-modified AuNPs. The DTT regulation procedure was performed as described above. After all immobilized probes were displaced from the particle surface, the unlabeled DNA strands (1X-DNA and SH-CBSA-SF) were collected from the supernatant after a 10-minute centrifugation at 25,000 rcf. The concentration of displaced probes was determined using OliGreen, a fluorescent dye that specifically labels single-stranded DNA. 10 mM Tris buffer (pH 7.4) was used to dilute 20 μL of the displaced DNA supernatant to 50 μL followed by addition of 50 μL of 1× OliGreen solution in 10 mM Tris buffer (pH 7.4). This mixture was incubated in the dark for 15 minutes, and then added into the wells of a 384-well plate. Fluorescence intensities were recorded at 525 nm (λ_{ex}= 500 nm). DNA surface coverage was determined by generating a standard curve by mixing 1× OliGreen solution with different concentrations of unlabeled DNA probe that had undergone the same DTT and centrifugation treatment.

Measuring effects of surface coverage on DNA detection in our colorimetric assay. We mixed 19 μL of the DTT-regulated, 1X-FAM-DNA or 1X-DNA modified-AuNPs (final concentration 5 nM) in 10 mM Tris buffer (pH 7.4) with 20 mM NaCl, 6 mM $MgCl_2$, and 1× BSA with 2 μL of DNA target (0, 10, 20, 35, 50, 100, 250, 500 and 1000 nM target for high-surface-coverage DNA-modified AuNPs; 0, 10, 15, 20, 35, 50, 100, 250, and 500 nM target for medium-surface-coverage DNA-modified AuNPs; and 0, 1, 5, 10, 15, 25, 50, 100 and 250 nM target for low-surface-coverage DNA-modified AuNPs). Upon addition of 4 μL Exo III (final concentration 0.05 U/μL), we recorded the absorbance over a range of 400–800 nm,

using A_{650}/A_{520} as a measure of the extent of aggregation. Sample images were obtained using a Canon Rebel T5 camera over a time span of 30 minutes.

Polyacrylamide gel electrophoresis (PAGE) characterization of Exo III digestion for the CBSA-cocaine complex. We tested Exo III-assisted target recycling using a cocaine-binding CBSA in solution. Briefly, 1 μL of CBSA-LF and 1 μL of CBSA-SF (final concentrations: 1 μM CBSA-LF, 1 or 8 μM CBSA-SF) were added to 38 μL of reaction buffer (final concentrations: 10 mM Tris, pH 7.4 and 0.1 mM $MgCl_2$). We then added 5 μL of cocaine (final concentration 250 μM) and incubated the mixture for 30 minutes, after which we added 5 μL of Exo III to the mixture (final concentration: 0.01 U/μL). 5 μL samples were collected at various time-points and mixed with 1× loading buffer (75% formamide, 0.02% SDS, 10% glycerol and 10 mM EDTA) to quench the digestion. The digestion products were separated on a 15% PAGE gel for three hours at 300 V. 1× SYBR Gold was used to stain the gel, and we characterized the cocaine-induced Exo III digestion based on the band intensity of CBSA-SF.

Assessing surface coverage effects on cocaine detection in our colorimetric assay. We resuspended the DTT-regulated, SH-CBSA-SF-modified AuNPs in buffer or 50% urine, with both containing 10 mM Tris (pH 7.4), 0.75 mM $MgCl_2$, 100 mM NaCl, 1× BSA and 100 nM CBSA-LF without or with cocaine (0, 0.25, 0.5, 1, 5 50, 100, 250 and 500 μM). After incubating for 30 minutes at room temperature, Exo III was added to the samples (final concentration 0.2 U/μL). Subsequently, the absorbance spectra from 400 to 800 nm were recorded and A_{650}/A_{520} was used to assess AuNP aggregation. Samples were imaged using a Canon Rebel T5 camera over a time span of 30 minutes.

RESULTS AND DISCUSSION

Using DTT to regulate surface coverage of DNA-conjugated AuNPs. We determined how DTT regulation affects the surface coverage of DNA-modified AuNPs by utilizing an AuNP-reported, EATR-based colorimetric assay targeting a complementary DNA sequence. Specifically, we designed a 46-nt DNA probe containing a three-carbon spacer abasic site (denoted by /iSpC3/) with the following sequence: 5'–poly(T_6)-ACCACATCATCC-/iSpC3/-TATAACTGAAAGCCAAACAG–3'. The probe DNA was modified with a 5' thiol group and a 3' FAM label to yield 1X-FAM-DNA. The 5' poly(T_6) serves a flexible linker which provides more distance between the recognition sequence and the AuNP surface, thereby improving both DNA hybridization and enzyme digestion. 1X-FAM-DNA was conjugated onto AuNPs via thiol-gold chemistry[29] at a 300:1 molar ratio, ensuring that the particles were saturated with DNA.

To regulate the surface coverage of these saturated 1X-FAM-DNA-modified AuNPs, we backfilled the particles with DTT. Previous work has shown that DTT adsorbs onto gold surfaces via both its thiol groups, orienting its two hydroxyl groups towards the solution.[28] We predicted that DTT would attach to the AuNP surface, displacing a subset of the immobilized 1X-FAM-DNA into solution, thereby allowing for regulation of DNA surface coverage (**Fig. 1**). AuNP conjugation quenches the fluorescence of FAM-labeled DNA, but that fluorescence is recovered upon detaching the DNA from the particle surface (**Fig. 1A**).[19] We therefore investigated the kinetics of DTT regulation of 1X-FAM-DNA-modified AuNPs by monitoring the recovery of FAM fluorescence. We mixed our 1X-FAM-DNA-modified AuNPs with DTT at a concentration range of 20–800 μM and recorded the fluorescence intensity of the samples over 60 minutes. Our experimental results demonstrated that the 1X-FAM-DNA probes were rapidly displaced

from the particle surface and released into solution upon addition of DTT, yielding increased fluoresence (**Fig. 1B**). DNA probe displacement began within 10 minutes, plateauing after 30 minutes (**Fig. 1B**). The level of DNA displacement was highly dependent on the DTT concentration. We noted that 1X-FAM-DNA-modified AuNPs treated with DTT concentrations greater than 800 μM underwent aggregation in the reaction buffer, when the particles no longer retained a sufficient number of DNA strands in order to maintain stable separation. We therefore omitted this treatment condition from further experiments. Our other DTT-treated AuNPs remained stable and well-dispersed.

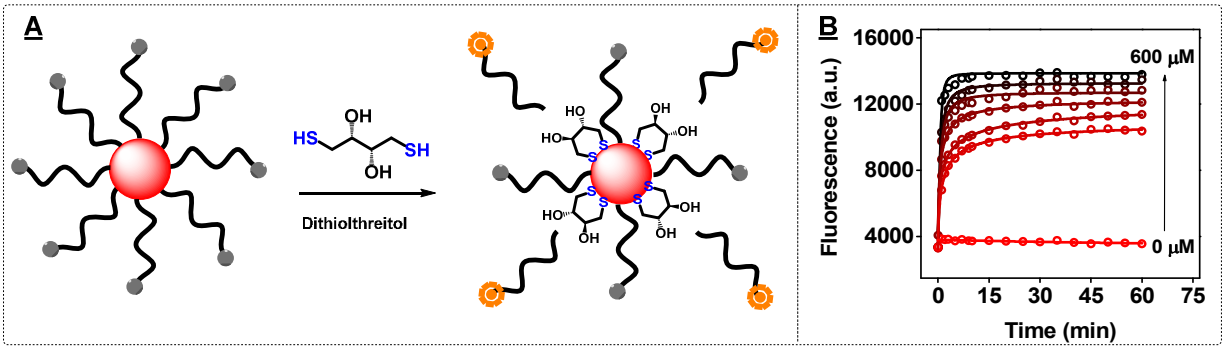

Figure 1. Using DTT to regulate DNA-modified AuNP surface coverage. (**A**) The DTT regulation procedure. (**B**) Kinetics of DTT regulation on 1X-FAM-DNA-modified AuNPs. DTT concentrations used were 0, 20, 40, 75, 150, 300, 450 and 600 μM.

To confirm whether DTT effectively regulated surface coverage on the AuNPs, we measured the surface coverage of DTT-treated AuNPs using a previously reported assay.[25] Specifically, we first mixed 1 M DTT with each batch of the DTT-regulated AuNPs in equal volumes, and then incubated for 16 hours to completely remove any remaining DNA strands. We then centrifuged the samples and measured the fluorescence of the collected supernatant. We constructed a calibration curve (**Supporting Information (SI), Fig. S1A**) to calculate the concentration of 1X-FAM-DNA probe in the supernatant and divided it by the concentration of AuNPs to obtain the DNA surface coverage. We determined that the fully-saturated 1X-FAM-DNA-modified AuNPs were modified with 120 strands/particle. Treatment with 20, 40, 75, 150, 300, 450 or 600 μM DTT produced lower coverages of 69±1, 53±1, 47±1, 39±1, 34±1, 30±1 and 26±1 strands/particle, respectively (**SI, Fig. S1B**). Clearly, DTT treatment rapidly regulated the DNA surface coverage of AuNPs in a concentration-dependent manner.

Assessing surface coverage effects on the kinetics of an AuNP-reported EATR-mediated assay for DNA detection. We subsequently demonstrated that the surface coverage of DNA has a profound effect on Exo III-mediated AuNP aggregation. To demonstrate this, we modified AuNPs with 1X-DNA probe which has the same sequence as 1X-FAM-DNA but does not contain the 3'-FAM label. These 1X-DNA-modified AuNPs were then regulated with DTT solutions of various concentrations and their surface coverages were measured using the displacement procedure described above. Since the 1X-DNA probes lack a fluorophore label, the concentration in the supernatant was measured using a fluorescent DNA-binding dye, Oligreen[33] (**SI, Fig. S2A**). 1X-DNA-modified AuNPs treated with 0, 10, 25, 50, 75, 100, 200 or 300 μM DTT exhibited coverage of 108±3, 88±1, 70±1, 60±1, 53±1, 48±1, 36±1 and 29±1 strands/particle, respectively (**SI, Fig. S2B**). AuNPs treated with DTT concentrations greater than 300 μM were unstable in the reaction buffer and were omitted from further experiments. In our experiments, we noticed that the same concentration of DTT displaced different quantities of 1X-FAM-DNA and 1X-

DNA. For example, 60.8% and 71.7% of 1X-FAM-DNA strands were removed by using 75 and 300 μM DTT, respectively. However, 50.9% and 73.1% 1X-DNA strands were respectively removed at the same DTT concentrations. We believe this discrepancy is due to batch-to-batch variation of AuNPs and the DTT stock used for experiments. To confirm this, we synthesized a new batch of 13-nm AuNPs and performed parallel modification with 1X-FAM-DNA and 1X-DNA under the same conditions. We measured surface coverage of 98 and 96 strands/particle for 1X-FAM-DNA and 1X-DNA, respectively, indicating that the FAM label has minimal effect on particle modification. We then incubated these modified AuNPs with concentrations of DTT ranging from 25 to 300 μM, which were prepared from the same DTT stock (**SI, Figs. S3A and S3B**). We observed similar DTT displacement efficiency for both sets of particles (**SI, Fig. S3C**), with only 7% and 3% more 1X-DNA strands displaced at 25 μM and 300 μM DTT, respectively, compared to 1X-FAM-DNA. We therefore believe that the FAM label has little effect on DTT displacement efficiency.

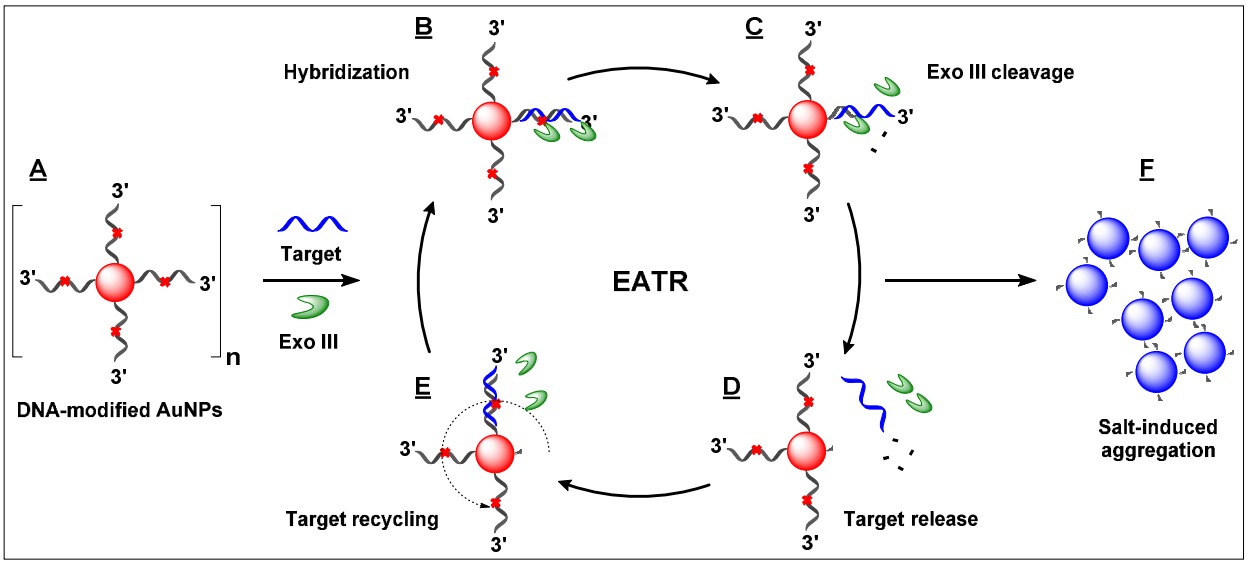

Figure 2. AuNP-reported, EATR-mediated colorimetric assay for DNA detection. (**A**) DNA-coated AuNPs remain stable in the solution. (**B**) Hybridization between the target DNA and the AuNP-conjugated probe forms a duplexed abasic site. (**C**) The duplexed abasic site is cleaved by Exo III, and then continues to digest the newly formed 3' hydroxyl group through its exonucleolytic activity. (**D**) The target DNA is released into solution (**E**) and recycled for subsequent hybridization and digestion, ultimately shearing all DNA from the AuNPs. (**F**) The sheared particles subsequently aggregate, causing the reaction solution to change color from red to blue.

We then tested the surface coverage effect in the context of an AuNP-reported, EATR-mediated assay for naked eye DNA detection (**Fig. 2**). Exo III cannot digest the single-stranded probes in the absence of the DNA target, such that the AuNPs stay separated and the solution remains red (**Fig. 2A**). If DNA target is present, a duplex is formed between the probe and the target (**Fig. 2B**). Exo III recognizes and generates a single-stranded nick at this duplexed abasic site via its apurinic endonucleolytic activity. The enzyme subsequently recognizes the resulting nick and proceeds to digest the nicked probe strand via its exonucleolytic activity (**Fig. 2C**). Once the immobilized probe DNA is cleaved from the particle surface, the DNA target is released into the solution (**Fig. 2D**) and then recycled to hybridize with another AuNP-bound probe DNA (**Fig. 2E**). Ultimately, all the surface-immobilized probe DNA strands will be digested. The sheared AuNPs eventually undergo aggregation, producing a red-to-blue color change (**Fig.**

2F). This process enables sensitive naked-eye detection of DNA, because of the signal amplification that results from the 'recycling' of a single target strand for the digestion of many probe strands.

We then performed time-dependent UV-vis measurements of 1X-DNA-modified AuNPs (**Fig. 3**), and used A_{650}/A_{520} to assess AuNP aggregation.[34] As DNA surface coverage was reduced, the initial value of A_{650}/A_{520} increased to 0.26 and 0.37 for AuNPs with 53 and 29 strands/particle, respectively, relative to a value of 0.19 for the fully-saturated 108 strands/particle AuNPs (**Fig. 3A, E**, and **H**). Although the stability of DTT-regulated AuNPs was slightly decreased, the particles still remained well-dispersed in solution, maintaining a red color ($A_{650}/A_{520} \leq 0.4$). Upon addition of Exo III, we observed that AuNPs with different surface coverages demonstrated various levels of Exo III-mediated AuNP aggregation after a 60-minute reaction. No aggregation was observed with non-regulated, DNA-saturated AuNPs (A_{650}/A_{520} = 0.20), even in the presence of DNA target (**Fig. 3A**). As surface coverage decreased, we observed a visible color shift from red (**Fig. 3B**, $A_{650}/A_{520} \leq 0.4$) to purple (**Figs. 3C** and **D**, $0.6 \leq A_{650}/A_{520} \leq 0.8$) and then to blue (**Figs. 3E, F, G**, and **H**, $A_{650}/A_{520} \geq 0.8$) in the presence of target. In contrast, solutions without target DNA remained red for the duration of the reaction.

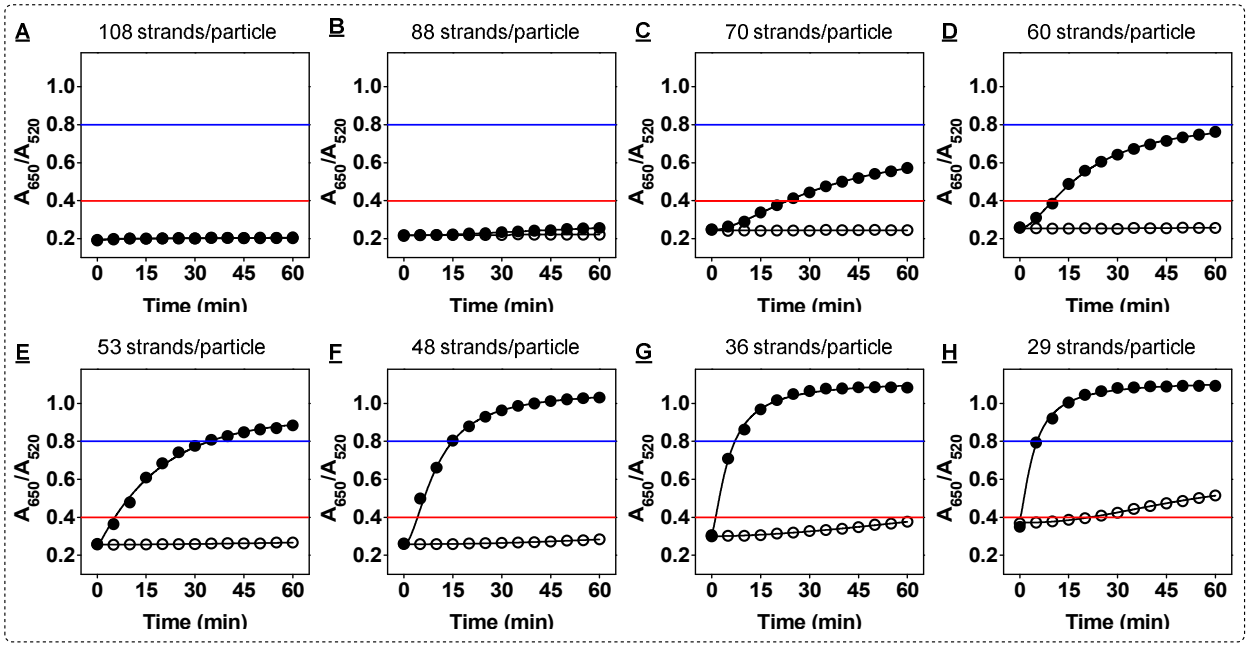

Figure 3. An EATR-mediated DNA detection assay utilizing DTT-regulated, 1X-DNA-modified AuNPs. Time-dependent measurement of A_{650}/A_{520} of AuNPs with (**A**) 108, (**B**) 88, (**C**) 70, (**D**) 60, (**E**) 53, (**F**) 48, (**G**) 36, and (**H**) 29 strands/particle. We performed Exo III digestion in the presence (solid circle) or absence (open circle) of 100 nM DNA target.

Reduction of surface coverage also greatly increased the reaction speed. Surface densities of 70, 60 and 53 strands/particle respectively achieved a purple color after 60, 27, and 17 minutes (**Figs. 3C, D** and **E**). The reaction times were even faster for AuNPs with lower surface coverages of 48, 36, and 29 strands/particle, which respectively produced a blue color within 17, 9, and 6 minutes (**Figs. 3F, G** and **H**), respectively. We believe that DTT regulation improves DNA hybridization and exonuclease digestion by fine-tuning the surface coverage of AuNPs. First, DTT prevents nonspecific adsorption of DNA onto the AuNP surface by occupying vacant areas on the particle surface. This lifts the covalently bound probe

strands into an upright orientation, easing DNA hybridization and increasing enzyme accessibility. Second, DTT treatment displaces some of the probe strands, thereby altering the final probe DNA density. This greatly attenuates the steric and electrostatic repulsion between neighboring DNA strands, which serves as a barrier for target and enzyme binding. Finally, decreased DNA surface coverage results in a lower amount of negatively charged phosphate groups present on the AuNP surface. This in turn decreases the local salt concentration, minimizing salt-induced exonuclease inhibition.

Effect of surface coverage on detection limit of our DNA detection assay. Having demonstrated that the degree of aggregation and reaction speed in the AuNP-reported EATR-mediated assay are dependent on the probe surface coverage, we subsequently examined the impact of this characteristic on the assay detection limit. We treated 1X-DNA-modified AuNPs with DTT to generate AuNPs with high (54±1 strands/particle), medium (43±1 strands/particle), and low (30±1 strands/particle) surface coverage and used them in a DNA detection assay with a reaction time of 20 minutes. At high surface coverage, we observed no red-to-blue color change at any DNA target concentration (**Fig. 4A**). However, we saw a red-to-purple color change for target concentrations ≥100 nM (**Fig. 4A** and **SI, Fig. S4A**). With medium surface coverage, we only observed a red-to-blue color change at target concentrations ≥250 nM (**Fig. 4B** and **SI, Fig. S4B**), although a color change from red to purple was observed at concentrations as low as 50 nM. At low surface coverage, a color change from red to blue occurred with 50 nM target, and a color change from red to purple was discernable with 15 nM target (**Fig. 4C** and **SI, Fig. S4C and Fig. S4D**). Thus, we have demonstrated that by using DTT to fine tune the surface coverage of DNA-modified AuNPs, one can improve the detection limit through enhanced target hybridization and enzyme digestion.

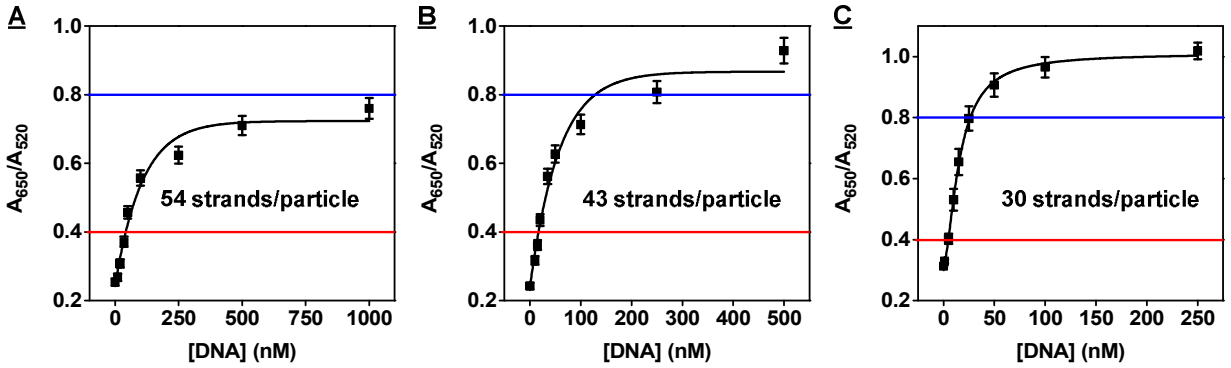

Figure 4. Calibration curves of DNA detection with DTT-regulated, 1X-DNA-modified AuNPs of varying coverage. Plots depict A_{650}/A_{520} after 20 minutes of reaction for (**A**) high, (**B**) medium, and (**C**) low surface coverage 1X-DNA-modified AuNPs challenged with various target concentrations.

DTT regulation of an AuNP-reported, EATR-mediated assay for the detection of cocaine. We then confirmed that the DTT regulation strategy is generalizable to other AuNP-based sensors. Specifically, we employed an EATR-mediated, AuNP-based assay that produces a colorimetric readout for the rapid, visual detection of cocaine, based on a highly target-responsive CBSA recently engineered by our group.[17] Our CBSA consists of a single pair of long (CBSA-LF) and short (CBSA-SF) fragments and contains dual target-binding domains upon assembly, with binding at the first site promoting tighter target binding at the second site. To facilitate Exo III digestion of the CBSA-cocaine complex, we incorporated a C3 apurinic site into CBSA-SF (**Fig. 5A, left**). Both fragments assemble via cooperative target binding in the presence of cocaine, forming the CBSA-cocaine complex (**Fig. 5A, right**). The duplexed apurinic

site is then nicked by Exo III, such that the long fragment and cocaine are released to achieve EATR. To confirm the selectivity of Exo III digestion, we incubated both CBSA fragments with Exo III with or without cocaine target and used polyacrylamide gel electrophoresis (PAGE) to characterize the digestion products (**Fig. 5B**). Specifically, we incubated 1 μM CBSA-LF and 1 μM CBSA-SF with or without 250 μM cocaine in binding buffer (10 mM Tris, 0.1 mM $MgCl_2$, and 1× BSA, pH 7.4) for 30 minutes, and then added Exo III to a final concentration of 0.01 U/μL. We collected samples and characterized digestion products from 0-, 5-, 10-, 15-, 30- and 60-minute time-points using 15% denaturing PAGE. We found that CBSA-SF was completely digested after 30 minutes in the presence of 250 μM cocaine, whereas 20% was digested in the absence of cocaine (**Fig. 5C**), indicating selective target-induced Exo III digestion.

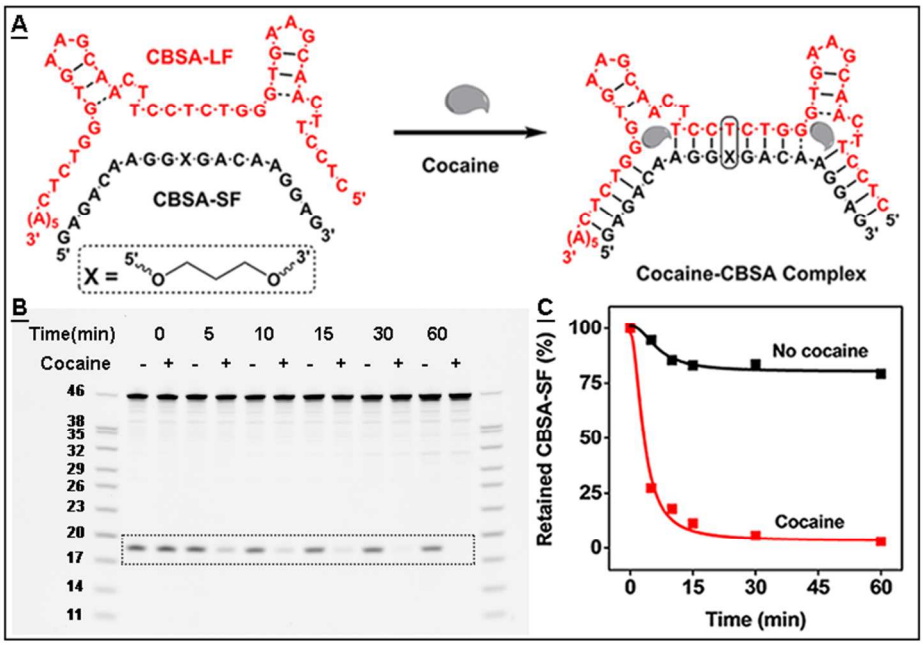

Figure 5. Specific digestion of cocaine-CBSA complexes by Exo III. (**A**) CBSA-SF and CBSA-LF remain separate when no cocaine is present. Cocaine promotes assembly of the short and long fragments, forming a duplexed apurinic site capable of being cleaved by Exo III. (**B**) PAGE analysis of CBSA digestion products with and without cocaine. (**C**) Percentage of intact CBSA-SF retained over the course of Exo III digestion.

We further demonstrated Exo III's ability to recycle cocaine and CBSA-LF over the course of an EATR reaction by performing Exo III digestion with 1 μM CBSA-LF and 8 μM CBSA-SF in the presence and absence of cocaine and characterizing the digestion products using PAGE (**SI, Fig. S5A**). Our results demonstrated that CBSA-SF was completely digested in 60 minutes in the presence of 250 μM cocaine, whereas only 20% was digested in the absence of cocaine (**SI, Fig. S5B**). This indicated that CBSA-LF and cocaine were released and recycled for multiple rounds of CBSA-cocaine assembly and Exo III digestion, thus achieving EATR. We also observed moderate digestion of CBSA-LF at its 3' terminus independent of whether cocaine was present or absent (**SI, Fig. S5A**), possibly due to non-specific 3'-to-5' exonuclease digestion by Exo III.[35]

Having successfully demonstrated the performance of our CBSA-based EATR assay for cocaine, we adapted this system into an AuNP-conjugated colorimetric assay (**Fig. 6**). We conjugated a thiolated version of CBSA-SF (SH-CBSA-SF) onto AuNPs, while the CBSA-LF remained free in solution. The

CBSA exists as two dissociated fragments in the absence of cocaine (**Fig. 6A**). Assembly of the CBSA on the AuNP only occurs when cocaine is present, forming a duplexed C3 apurinic site (**Fig. 6B**). Exo III then initiates apurinic endonucleolytic cleavage (**Fig. 6C**), dissociating the cleaved strand from the complex and releasing CBSA-LF and cocaine into the solution (**Fig. 6D**). The released cocaine and CBSA-LF can then associate with another SH-CBSA-SF immobilized on the same or a different AuNP to assemble a new CBSA-cocaine complex, initiating another round of EATR (**Fig. 6E**). After multiple rounds of CBSA assembly and EATR, all immobilized SH-CBSA-SF strands have been removed from the particle. These particles subsequently aggregate due to the high salt concentration of the buffer, producing a color change (**Fig. 6F**). If cocaine is not present, the CBSA fragments fail to assemble, Exo III cannot recognize and digest the single-stranded SH-CBSA-SF, and the solution remains red.

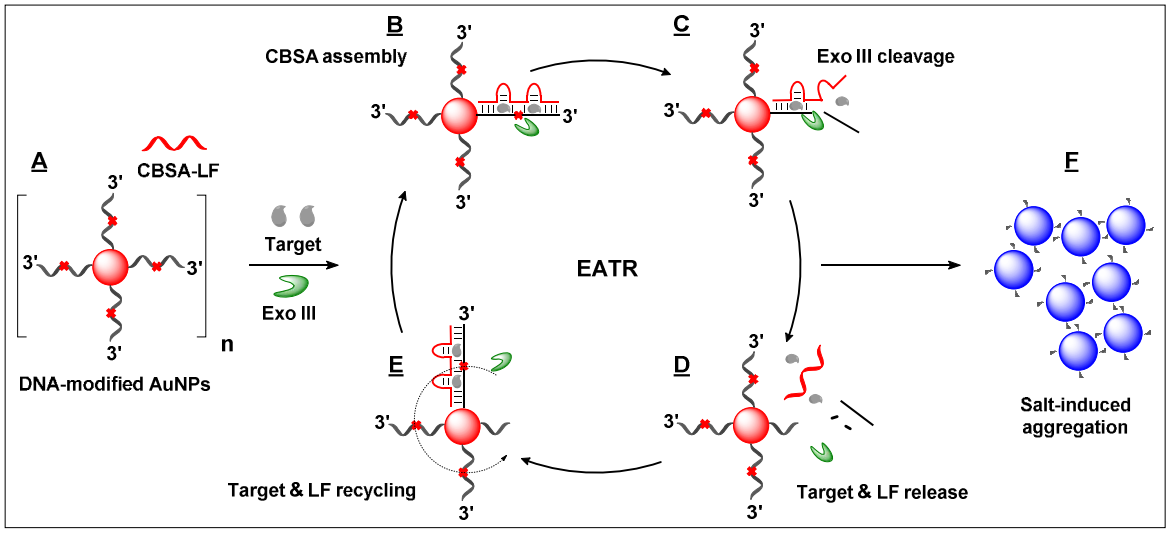

Figure 6. AuNP-reported, EATR-mediated colorimetric assay for cocaine detection. (**A**) SH-CBSA-SF is conjugated to AuNPs while the long fragment remains free in solution. (**B**) Cocaine mediates CBSA assembly on the particle surface, forming a duplexed abasic site. (**C**) Exo III's endonucleolytic apurinic activity cleaves the duplexed abasic site. (**D**) The CBSA-LF and cocaine are then released into solution (**E**) and recycled for subsequent CBSA assembly and Exo III digestion, ultimately shearing all DNA from the particle and (**F**) producing a red-to-blue color change.

Assessing the effect of DNA surface coverage on cocaine detection. We prepared SH-CBSA-SF-modified AuNPs using the protocol described above with a molar ratio of SH-CBSA-SF to AuNP of 300 to obtain saturated surface coverage. We then measured the DNA surface coverage as described for the 1X-DNA-modified AuNPs, and determined that the saturated AuNPs displayed 78±2 strands/particle. We then performed an EATR-based colorimetric assay in 25 µL of reaction buffer plus 100 nM CBSA-LF, 5 nM SH-CBSA-SF-modified AuNPs, and 0.2 U/µL Exo III with or without 250 µM target. The AuNPs were well-dispersed, and the solution remained red (A_{650}/A_{520} = 0.25) after a 60-minute digestion, regardless of the absence or presence of cocaine (**Fig. 7A**). The solution color remained red even after an overnight incubation (data not shown). This suggests that the steric and electrostatic repulsive forces between the SH-CBSA-SF strands may have interrupted cocaine-induced assembly and/or reduced Exo III access to cleavage sites at the AuNP surface. Similar to our DNA assay, the surface coverage of aptamer-modified AuNPs strongly affects assembly of aptamer-target complexes, Exo III digestion, and AuNP aggregation. To achieve successful EATR, we used DTT to reduce the surface coverage of SH-

CBSA-SF. AuNPs incubated with DTT at concentrations >200 μM aggregated, and were omitted from further experiments. After a 30-minute reaction, the displaced SH-CBSA-SF and excess DTT were removed from the samples through centrifugation, and the particles were washed and dissolved in 10 mM Tris buffer (pH 7.4). Based on an OliGreen-constructed calibration curve (**SI, Fig. S6A**), we found that the SH-CBSA-SF-modified AuNPs regulated with DTT concentrations of 0, 25, 50, 75, 100, 150, 165, 180, and 200 μM respectively displayed 78±2, 50±1, 45±1, 42±1, 40±1, 37±1, 34±1, and 33±1 strands/particle (**SI, Fig. S6B**).

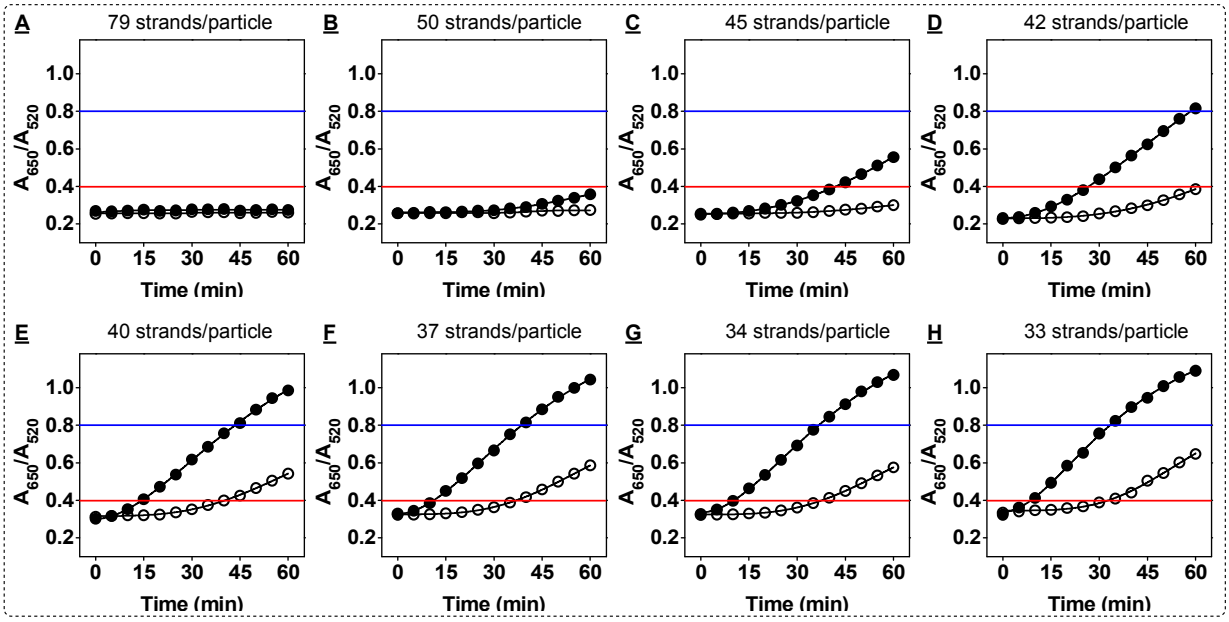

Figure 7. Exo III digestion of AuNP-conjugated SH-CBSA-SF for cocaine detection. Time-dependent measurement of A_{650}/A_{520} for AuNPs with surface coverage of (**A**) 79, (**B**) 50, (**C**) 45, (**D**) 42, (**E**) 40, (**F**) 37, (**G**) 34 and (**H**) 33 strands/particle. Exo III digestion of AuNP-conjugated SH-CBSA-SF was performed with (solid circle) or without (open circle) of 250 μM cocaine.

We used these DTT-regulated AuNPs to perform our EATR-mediated colorimetric cocaine detection assay. At high surface coverage (50 strands/particle), the solution remained red after a 60-minute reaction (**Fig. 7B**). Reduction in surface coverage increased the reaction speed, with medium-to-low surface coverages yielding a clear colorimetric readout in the presence of cocaine. Specifically, the 45 strands/particle AuNPs generated a red-to-purple color change after 1 hour (**Fig. 7C**). The 42 strands/particle AuNPs achieved a red-to-purple color change in 44 minutes, and a red-to-blue color change in approximately 60 minutes (**Fig. 7D**). AuNPs with surface coverages of 40, 37, 34, and 33 strands/particle produced a red-to-blue color change after 44, 39, 33, 30 minutes, respectively (**Figs 7E–H**). We therefore conclude that DTT regulation promotes EATR in this cocaine-detection assay through similar mechanisms to those described in our DNA detection assay above.

In order to evaluate our assay's sensitivity, we derived calibration curves from SH-CBSA-SF-modified AuNPs with high (50 strands/particle), medium (40 strands/particle), and low (33 strands/particle) surface coverage. AuNPs with high surface coverage remained red in the presence of up to 500 μM cocaine after 60 minutes of reaction, indicating strong inhibition of CBSA assembly and Exo III digestion (**SI, Fig.**

S7A and **D**). AuNPs with medium surface coverage produced less inter-strand repulsion and provided more space for CBSA-based EATR, generating a red-to-purple color change with 5–50 μM cocaine and a red-to-blue color change with 100–500 μM cocaine after 60 minutes (**SI, Fig. S7B** and **D**). Low surface coverage AuNPs favored EATR even more, yielding similar color-changes to various concentrations of cocaine as the medium surface coverage particles but within half the time (**SI, Fig. S7C** and **D**). A red-to-purple color change could readily be observed by naked eye with 5 μM cocaine in these low surface-coverage samples after only 30 minutes. Thus, reducing surface coverage using DTT offers a general strategy for greatly decreasing the assay reporting time and increasing the detection limit in AuNP-based biosensing assays. The robustness of our AuNP-reported, EATR-mediated colorimetric assay should enable rapid cocaine detection, even in complex biological samples. To demonstrate this, we spiked various concentrations of cocaine into urine and tested the samples with our assay. After a 30-minute Exo III digestion, we found that concentrations as low as 5 μM cocaine in 50% urine could be distinguished by the naked eye (**SI, Figure S8**). We determined that the multitude of endogenous compounds in urine did not interfere with the assay.

CONCLUSION

Current methods for regulating the surface coverage of DNA-modified AuNPs require preparation of multiple batches of AuNPs under different conditions, which is costly and laborious. We here used DTT to rapidly regulate the surface coverage of AuNPs from a single batch of DNA-modified AuNPs with saturated surface coverage in a single step. We demonstrated that DTT regulation of surface coverage greatly improved the performance of DNA-modified AuNP-based assays for detecting both DNA and small-molecule targets.

We specifically selected DTT as a surface diluent to optimize AuNP-based biosensors due to several reasons. First, DTT is less volatile than other commonly used alkanethiol diluents such as mercaptohexanol (MCH), therefore, low concentrations of DTT can be prepared and used to reproducibly fine-tune the surface coverage of AuNPs. Compared with millimolar concentrations and 1 to 12 hours of incubation required for MCH backfilling,[19,22] DTT at micromolar concentrations rapidly occupies vacancies on the gold surface and also displaces a portion of immobilized DNA probes within 30 minutes in a concentration-dependent manner. Second, it has been shown that surface-bound bidentate alkanethiols, such as DTT, are much less susceptible to spontaneous desorption and are more resistant to displacement by competing thiolated compounds than their monodentate counterparts.[36–39] Third, since endogenous thiol-containing compounds such as glutathione cannot efficiently displace even monodentate thiols from the surface of AuNPs at physiological concentrations,[40] surface-bound DTT should be stable in biosamples. Fourth, given that DTT can pack at higher densities on gold surfaces compared with MCH,[41,42] less non-specific adsorption of DNA probes and greater anti-fouling abilities can be observed with DTT-treated surfaces.[43,44] This was demonstrated using DTT as a backfiller, which allowed for the successful electrochemical detection of targets such as thrombin and adenosine in serum.[43,44]

In this work, we elucidated the impact of DTT on sensor performance with an AuNP-reported, EATR-based assay for colorimetric DNA detection. We determined that reduced surface coverage resulted in accelerated aggregation and lower detection limits, enabling visual detection of target DNA concentrations as low as 5 nM within 20 minutes. Based on previous works,[45,46] we believe that the detection limit of this assay could be lowered by performing Exo III digestion at 4 °C for 12 hours. In

contrast, DNA-saturated AuNPs did not generate a target-induced readout due to the effects of excessively high surface coverage. We also confirmed that our DTT regulation method is compatible with an AuNP-reported, EATR-based assay for small-molecule detection, which employed a previously engineered cocaine-binding CBSA. As with our DNA assay, reduction of surface coverage on the AuNPs dramatically increased the reaction speed and greatly improved sensitivity, enabling colorimetric detection of 50 μM cocaine in buffer within only 30 minutes. We also demonstrated the practical use of DTT-treated, DNA-modified-AuNPs in biological samples by performing low micromolar cocaine detection in 50% urine and observed minimal matrix effects on assay sensitivity. It should be noted that the colorimetric readouts for all assays could also be qualitatively assessed by naked eye, without the need for instrumental analysis. Our DTT regulation method is simple, fast, and reproducible, and we believe it should be useful for fine-tuning the surface coverage of oligonucleotide-modified AuNPs for the colorimetric detection of a multitude of targets. We further believe that our method can be used to optimize AuNP performance in other applications, such as drug delivery and therapeutic treatment, in which surface coverage may profoundly influence function.

ASSOCIATED CONTENT

Supporting information (SI) available: The supporting information is available free of charge on the ACS Publications website. DTT-regulated surface coverage of 1X-FAM-DNA-modified AuNPs; DTT-regulated surface coverage of 1X-DNA-modified AuNPs; comparison of DTT regulation of 1X-DNA-modified and 1X-FAM-DNA-modified AuNPs prepared with the same batch of AuNPs and DTT stock; calibration curves of DTT-regulated 1X-DNA-modified AuNPs with high (54 strands/particle), medium (43 strands/particle), and low (30 strands/particle) surface coverage; recycling of CBSA-LF and cocaine in our EATR assay; DTT-regulated surface coverage of SH-CBSA-SF-modified AuNPs; calibration curves of SH-CBSA-SF-modified AuNPs with various surface coverages; calibration curve of DTT-regulated SH-CBSA-SF-modified AuNPs in 50% urine for cocaine detection.

AUTHOR INFORMATION

Corresponding Author

*E-mail addresses: yxiao2@fiu.edu. Tel: 305-348-4536

Notes

The authors declare no competing financial interest.

ACKNOWLEDGEMENTS

This work was supported by the National Institutes of Health – National Institute on Drug Abuse [R15DA036821] and Florida International University Dissertation Year Fellowship.

REFERENCES

(1) Luo, X.; Morrin, A.; Killard, A. J.; Smyth, M. R. Application of Nanoparticles in Electrochemical Sensors and Biosensors. *Electroanalysis* **2006**, *18*, 319–326.

(2) Zhao, W.; Brook, M. A.; Li, Y. Design of Gold Nanoparticle-Based Colorimetric Biosensing Assays. *ChemBioChem* **2008**, *9*, 2363–2371.

(3) Thaxton, C. S.; Georganopoulou, D. G.; Mirkin, C. A. Gold Nanoparticle Probes for the Detection of Nucleic Acid Targets. *Clin. Chim. Acta* **2006**, *363*, 120–126.

(4) Prigodich, A. E.; Randeria, P. S.; Briley, W. E.; Kim, N. J.; Daniel, W. L.; Giljohann, D. A.; Mirkin, C. A. Multiplexed Nanoflares: mRNA Detection in Live Cells. *Anal. Chem.* **2012**, *84*, 2062–2066.

(5) Storhoff, J. J.; Lucas, A. D.; Garimella, V.; Bao, Y. P.; Müller, U. R. Homogeneous Detection of Unamplified Genomic DNA Sequences Based on Colorimetric Scatter of Gold Nanoparticle Probes. *Nat. Biotechnol.* **2004**, *22*, 883–887.

(6) Prigodich, A. E.; Seferos, D. S.; Massich, M. D.; Giljohann, D. A.; Lane, B. C.; Mirkin, C. A. Nano-Flares for mRNA Regulation and Detection. *ACS Nano* **2009**, *3*, 2147–2152.

(7) Park, S. Y.; Lytton-Jean, A. K. R.; Lee, B.; Weigand, S.; Schatz, G. C.; Mirkin, C. A. DNA-Programmable Nanoparticle Crystallization. *Nature* **2008**, *451*, 553–556.

(8) De, M.; Ghosh, P. S.; Rotello, V. M. Applications of Nanoparticles in Biology. *Adv. Mater* **2008**, *20*, 4225–4241.

(9) Jin, R.; Wu, G.; Li, Z.; Mirkin, C. A.; Schatz, G. C. What Controls the Melting Properties of DNA-Linked Gold Nanoparticle Assemblies? *J. Am. Chem. Soc.* **2003**, *125*, 1643–1654.

(10) Storhoff, J. J.; Lazarides, A. A.; Mucic, R. C.; Mirkin, C. A.; Letsinger, R. L.; Schatz, G. C. What Controls the Optical Properties of DNA-Linked Gold Nanoparticle Assemblies? *J. Am. Chem. Soc.* **2000**, *122*, 4640–4650.

(11) Zhao, W.; Lam, J. C. F.; Chiuman, W.; Brook, M. A.; Li, Y. Enzymatic Cleavage of Nucleic Acids on Gold Nanoparticles: A Generic Platform for Facile Colorimetric Biosensors. *Small* **2008**, *4*, 810–816.

(12) Xu, X.; Han, M. S.; Mirkin, C. A. A Gold-Nanoparticle-Based Real-Time Colorimetric Screening Method for Endonuclease Activity and Inhibition. *Angew. Chem., Int. Ed.* **2007**, *46*, 3468-3470.

(13) Liu, T.; Zhao, J.; Zhang, D.; Li, G. Novel Method to Detect DNA Methylation Using Gold Nanoparticles Coupled with Enzyme-Linkage Reactions. *Anal. Chem.* **2010**, *82*, 229–233.

(14) Wu, S.; Liang, P.; Yu, H.; Xu, X.; Liu, Y.; Lou, X.; Xiao, Y. Amplified Single Base-Pair Mismatch Detection via Aggregation of Exonuclease-Sheared Gold Nanoparticles. *Anal. Chem.* **2014**, *86*, 3461-3467.

(15) Tuerk, C.; Gold, L. Systematic Evolution of Ligands by Exponential Enrichment: RNA Ligands to Bacteriophage T4 DNA Polymerase. *Science* **1990**, *249*, 505–510.

(16) Ellington, A. D.; Szostak, J. W. *In Vitro* Selection of RNA Molecules That Bind Specific Ligands. *Nature* **1990**, *346*, 818–822.

(17) Yu, H. X.; Canoura, J.; Guntupalli, B.; Lou, X. H.; Xiao, Y. A Cooperative-Binding Split Aptamer Assay for Rapid, Specific and Ultra-Sensitive Fluorescence Detection of Cocaine in Saliva. *Chem. Sci.* **2017**, *8*, 131–141.

(18) Brown, K. A.; Park, S.; Hamad-Schifferli, K. Nucleotide-Surface Interactions in DNA-Modified Au-Nanoparticle Conjugates : Sequence Effects on Reactivity and Hybridization. *J. Phys. Chem. C* **2008**, 120, 7517–7521.

(19) Demers, L. M.; Mirkin, C. A.; Mucic, R. C.; Reynolds, R. A.; Letsinger, R. L.; Elghanian, R.; Viswanadham, G. A Fluorescence-Based Method for Determining the Surface Coverage and Hybridization Efficiency of Thiol-Capped Oligonucleotides Bound to Gold Thin Films and Nanoparticles. *Anal. Chem.* **2000**, *72*, 5535–5541.

(20) Nicewarner Peña, S. R.; Raina, S.; Goodrich, G. P.; Fedoroff, N. V.; Keating, C. D. Hybridization and Enzymatic Extension of Au Nanoparticle-Bound Oligonucleotides. *J. Am. Chem. Soc.* **2002**,

124, 7314–7323.

(21) Lee, C.; Gong, P.; Harbers, G. M.; Grainger, D. W.; Castner, D. G.; Gamble, L. J. Surface Coverage and Structure of Mixed DNA/Alkylthiol Monolayers on Gold : Characterization by XPS, NEXAFS, and Fluorescence Intensity Measurements. *Anal. Chem.* **2006**, *78*, 3316–3325.

(22) Herne, T. M.; Tarlov, M. J. Characterization of DNA Probes Immobilized on Gold Surfaces. *J. Am. Chem. Soc.* **1997**, *119*, 8916–8920.

(23) Rant, U.; Arinaga, K.; Fujita, S.; Yokoyama, N.; Abstreiter, G.; Tornow, M. Structural Properties of Oligonucleotide Monolayers on Gold Surfaces Probed by Fluorescence Investigations. *Langmuir* **2004**, *20*, 10086–10092.

(24) Seferos, D. S.; Prigodich, A. E.; Giljohann, D. A.; Patel, P. C.; Mirkin, C. A. Polyvalent DNA Nanoparticle Conjugates Stabilize Nucleic Acids. *Nano Lett.* **2009**, *9*, 308–311.

(25) Hurst, S. J.; Lytton-Jean, A. K. R.; Mirkin, C. A. Maximizing DNA Loading on a Range of Gold Nanoparticle Sizes. *Anal. Chem.* **2006**, *78*, 8313–8318.

(26) Storhoff, J. J.; Elghanian, R.; Mucic, R. C.; Mirkin, C. A.; Letsinger, R. L. One-Pot Colorimetric Differentiation of Polynucleotides with Single Base Imperfections Using Gold Nanoparticle Probes. *J. Am. Chem. Soc.* **1998**, *120*, 1959–1964.

(27) Tsai, D.; Cho, T. J.; Delrio, F. W.; Gorham, J. M.; Zheng, J.; Tan, J.; Zachariah, M. R.; Hackley, V. A. Controlled Formation and Characterization of Dithiothreitol-Conjugated Gold Nanoparticle Clusters. *Langmuir* **2014**, *30*, 3397-3405.

(28) MacDairmid, A. R.; Gallagher, M. C.; Banks, J. T. Structure of Dithiothreitol Monolayers on Au(111). *J. Phys. Chem. B* **2003**, *107*, 9789–9792.

(29) Mirkin, C. A.; Letsinger, R. L.; Mucic, R. C.; Storhoff, J. J. A DNA-Based Method for Rationally Assembling Nanoparticles into Macroscopic Materials. *Nature* **1996**, *382*, 607–609.

(30) Grabar, K. C.; Freeman, R. G.; Hommer M. B.; Natan, M.J. Preparation and Characterization of Au Colloid Monolayers. *Anal. Chem.* **1995**, *67*, 735–743.

(31) Jain, P. K.; Lee, K. S.; El-Sayed, I. H.; El-Sayed, M. A. Calculated Absorption and Scattering Properties of Gold Nanoparticles of Different Size, Shape, and Composition: Applications in Biological Imaging and Biomedicine. *J. Phys. Chem B* **2006**, *110*, 7238–7248.

(32) Nanodots, S.; Link, S.; El-sayed, M. A. Spectral Properties and Relaxation Dynamics of Surface Plasmon Electronic Oscillations in Gold and Silver Nanodots and Nanorods. *J. Phys. Chem. B* **1999**, *103*, 8410–8426.

(33) Mansfield, E. S.; Worley, J. M.; Mckenzie, S. E.; Surrey, S.; Rappaport, E.; Fortina, P. Nucleic Acid Detection Using Non-Radioactive Labelling Methods. *Mol. Cell. Probes* **1995**, *9*,145–156.

(34) Link, S.; El-Sayed, M. A. Size and Temperature Dependence of the Plasmon Absorption of Colloidal Gold Nanoparticles. *J. Phys. Chem. B* **1999**, *103*, 4212–4217.

(35) Shida, T.; Noda, M.; Sekiguchi, J. Cleavage of Single- and Double-Stranded DNAs Containing an Abasic Residue by *Escherichia Coli* Exonuclease III (AP Endonuclease VI). *Nucleic Acids Res.* **1996**, *24*, 4572–4576.

(36) Creczynski-Pasa, T. B.; Millone, M. A. D.; Munford, M. L.; de Lima, V. R.; Vieira, T. O.; Benitez, G. A; Pasa, A. A; Salvarezza, R. C.; Vela, M. E. Self-Assembled Dithiothreitol on Au Surfaces for Biological Applications: Phospholipid Bilayer Formation. *Phys. Chem. Chem. Phys.* **2009**, *11*, 1077–1084.

(37) Esplandiu, M. J.; Carot, M. L.; Cometto, F. P.; MacAgno, V. A.; Patrito, E. M. Electrochemical STM Investigation of 1,8-Octanedithiol Monolayers on Au(111).: Experimental and Theoretical Study. *Surf. Sci.* **2006**, *600*, 155–172.

(38) Schulz, F.; Vossmeyer, T.; Bastús, N. G.; Weller, H. Effect of the Spacer Structure on the Stability of Gold Nanoparticles Functionalized with Monodentate Thiolated Poly(ethylene glycol) Ligands. *Langmuir* **2013**, *29*, 9897–9908.

(39) Lee, H. J.; Jamison, A. C.; Yuan, Y.; Li, C. H.; Rittikulsittichai, S.; Rusakova, I.; Lee, T. R. Robust Carboxylic Acid-Terminated Organic Thin Films and Nanoparticle Protectants Generated from Bidentate Alkanethiols. *Langmuir* **2013**, *29*, 10432–10439.

(40) Han, G.; Chari, N. S.; Verma, A.; Hong, R.; Martin, C. T.; Rotello, V. M. Controlled Recovery of the Transcription of Nanoparticle-Bound DNA by Intracellular Concentrations of Glutathione. *Bioconjugate Chem.* **2005**, *16*, 1356–1359.

(41) Kuralay, F.; Campuzano, S.; Haake, D. A.; Wang, J. Highly Sensitive Disposable Nucleic Acid Biosensors for Direct Bioelectronic Detection in Raw Biological Samples. *Talanta* **2011**, *85*, 1330–1337.

(42) Wu, J.; Campuzano, S.; Halford, C.; Haake, D. A.; Wang, J. Ternary Surface Monolayers for Ultrasensitive (Zeptomole) Amperometric Detection of Nucleic Acid Hybridization without Signal Amplification. *Anal. Chem.* **2010**, *82*, 8830–8837.

(43) Qi, H.; Shangguan, L.; Li, C.; Li, X.; Gao, Q.; Zhang, C. Sensitive and Antifouling Impedimetric Aptasensor for the Determination of Thrombin in Undiluted Serum Sample. *Biosens. Bioelectron.* **2013**, *39*, 324–328.

(44) Wang, Y.; Feng, J.; Tan, Z.; Wang, H. Electrochemical Impedance Spectroscopy Aptasensor for Ultrasensitive Detection of Adenosine with Dual Backfillers. *Biosens. Bioelectron.* **2014**, *60*, 218–223.

(45) Zuo, X. L.; Xia, F.; Xiao, Y.; Plaxco, K. W. Sensitive and Selective Amplified Fluorescence DNA Detection Based on Exonuclease III-Aided Target Recycling. *J. Am. Chem. Soc.* **2010**, *132*, 1816–1818.

(46) Wu, S.; Liang, P. P.; Yu, H. X.; Xu, X. W.; Liu, Y.; Lou, X. H.; Xiao, Y. Amplified Single Base-Pair Mismatch Detection via Aggregation of Exonuclease-Sheared Gold Nanoparticles. *Anal. Chem.* **2014**, *86*, 3461–3467.

TOC

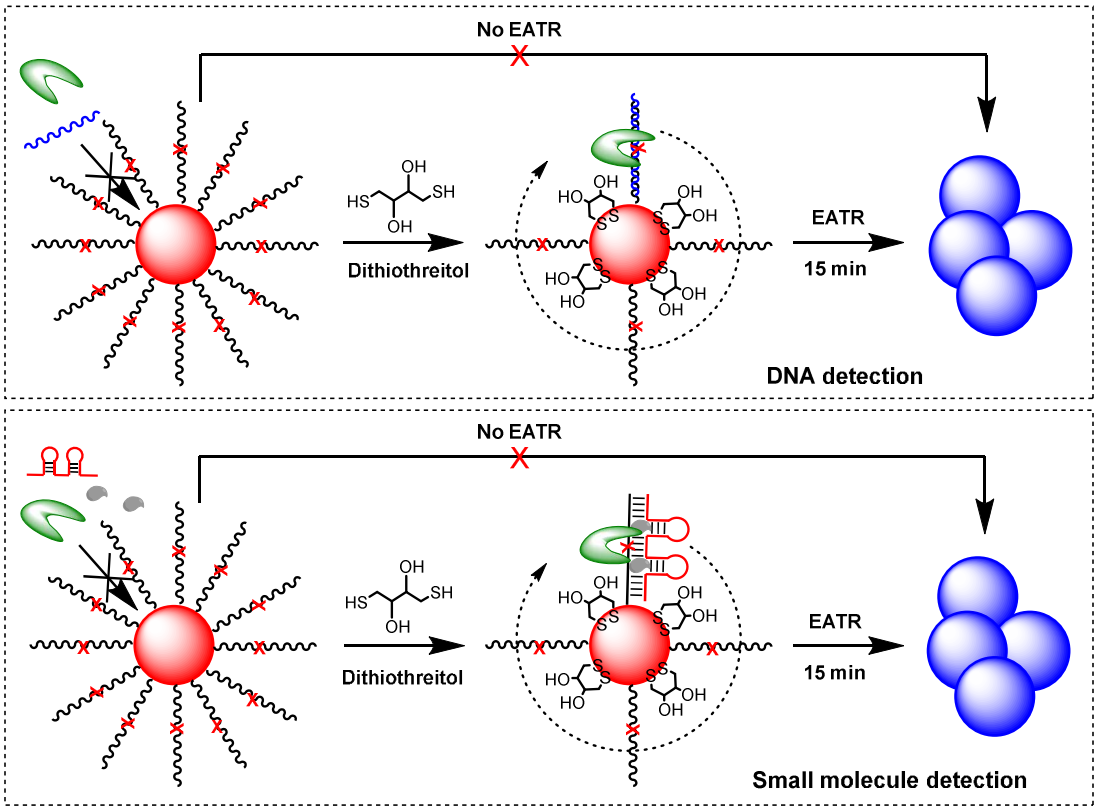
No EATR
Dithiothreitol
EATR
15 min
DNA detection
No EATR
Dithiothreitol
EATR
15 min
Small molecule detection